Hindawi
Advances in Materials Science and Engineering
Volume 2023, Article ID 9798764, 1 page
https://doi.org/10.1155/2023/9798764

*Retraction*

# Retracted: Influence of Metallic Particles on Properties of Aluminium Composites through Taguchi Technique

**Advances in Materials Science and Engineering**

Received 26 December 2023; Accepted 26 December 2023; Published 29 December 2023



This article has been retracted by Hindawi, as publisher, following an investigation undertaken by the publisher [1]. This investigation has uncovered evidence of systematic manipulation of the publication and peer-review process. We cannot, therefore, vouch for the reliability or integrity of this article.

Please note that this notice is intended solely to alert readers that the peer-review process of this article has been compromised.

Wiley and Hindawi regret that the usual quality checks did not identify these issues before publication and have since put additional measures in place to safeguard research integrity.

We wish to credit our Research Integrity and Research Publishing teams and anonymous and named external researchers and research integrity experts for contributing to this investigation.

The corresponding author, as the representative of all authors, has been given the opportunity to register their agreement or disagreement to this retraction. We have kept a record of any response received.

## References

[1] B. Venkatesh, A. R. Lakshmipathi, T. Prakash et al., "Influence of Metallic Particles on Properties of Aluminium Composites through Taguchi Technique," *Advances in Materials Science and Engineering*, vol. 2023, Article ID 9637728, 12 pages, 2023.

Hindawi
Advances in Materials Science and Engineering
Volume 2023, Article ID 9637728, 12 pages
https://doi.org/10.1155/2023/9637728



*Research Article*

# Influence of Metallic Particles on Properties of Aluminium Composites through Taguchi Technique

**B. Venkatesh,[1] Anantha Raman Lakshmipathi,[2] T. Prakash,[3] Pothamsetty Kasi V. Rao,[4] Rajesh Verma,[5] N. Nagabhooshanam,[6] and Simon Yishak [7]**

[1]*Department of Mechanical Engineering, Vardhaman College of Engineering, Hyderabad, Telangana, India*
[2]*Department of Mechanical Engineering, Madanapalle Institute of Technology and Science, Madanapalle, Andhra Pradesh, India*
[3]*Department of Mechanical Engineering, SNS College of Technology, Coimbatore 641035, Tamil Nadu, India*
[4]*Department of Mechanical Engineering, Koneru Lakshmaiah Education Foundation, Vaddeswaram, Andhra Pradesh, India*
[5]*Department of Electrical Engineering, College of Engineering, King Khalid University, Abha, Saudi Arabia*
[6]*Department of Mechanical Engineering, Aditya Engineering College, Surampalem 533437, Andhra Pradesh, India*
[7]*College of Engineering and Argo-Industrial Technology, Sawla Campus, Arba Minch University, Arba Minch, Ethiopia*

Correspondence should be addressed to Simon Yishak; simon.yishak@amu.edu.et

Received 27 June 2022; Revised 20 August 2022; Accepted 8 September 2022; Published 10 May 2023

Academic Editor: K. Raja



In this work, aluminium composites have been evaluated in terms of their characteristics and behaviour. Stirring metallics and a specific quantity of ceramic-derived silicon nitride resulted in AA6061 composites ($Si_3N_4$). The mechanical, corrosion, and tribological properties of composites were investigated. Tensile, corrosion, and hardness characteristics have been improved in composites with a constant weight percent of ceramic and advanced metallic fortification. The improved hardness of the composite has decreased wear and friction. Furthermore, by using ceramic strengthening with the metal, the impact strength of the composites was condensed. In addition to the research, the design of experiments method was used to optimize the important wear test elements such as reinforcement %, applied stress, sliding distance, and speed. Analysis of variance was used to find the most significant testing features and its interface with wear performance and the friction coefficient of the composite specimen.

## 1. Introduction

Two or more separate materials are combined in a composite material, which has an identifiable interface between the two [1]. The ability to combine characteristics in conventional monolithic materials is constrained. Composites, on the other hand, have been built for increased particular stiffness and specific strength, wear and fatigue resistance, creep and corrosion resistance, as well as a variety of other advantages [2, 3]. To achieve these features, the volume fraction of strengthening can be controlled, and the desired amount of strength and stiffness can be selected for the reinforcements. Composites are accessible in a variety of forms in today's competitive market. MMCs (metal-metal-ceramic-ceramic) are only a few examples, but there are many more (PMCs). As a result of their high hardness and operating performance, MMCs play a key role in the industrial sector [4–6]. Reinforcement phases can be added to MMCs using one or more of the following methods: spray and codeposition, powder metallurgy, thermal spraying, LMR, and compacted techniques, such as squeeze casting, or a combination of these techniques. As a result of its affordability, stir casting remains a popular manufacturing technology [7]. Stirrer motion guarantees that reinforcement is evenly distributed throughout the matrix, and material is able to accept reinforcement and volume by 30%. The possibility of obtaining the required materials is an additional benefit [8, 9]. A surge in the usage of lighter materials in manufacturing is owing to the higher strength-to-weight ratio, simple fabrication, and rate reductions associated with MMCs composites. As a result of the rise of globalisation and the improvement of production, alloys are ideal lightweight

materials [10–14]. As a result, there is a great need for structures that are both strong and light in weight. Boron carbide, silicon carbide, alumina, and other ceramic-based reinforcements are among the most often employed in the current market for MMCs' reinforcement [15].

The research presented here shows that composites based on aluminium AA6082 with silicon nitride reinforcement have been created [16, 17]. It is a sign that adding reinforcement has improved the material's density and porosity. Additionally, composites have gained in hardness and tensile strength. More than two reinforcements in the matrix gave rise to the name "hybrid composite," and one study examined a hybrid composite consisting of 1.0 volume% Silicon Carbide and 0.5 vol. % Boron Carbide [18–20]. There is a minor reduction in impact strength with this percentage and combination of hardness and tensile strength. All important structural applications in automotive manufacturing have been served by AA7075, a 7-series aluminium alloy [21, 22]. According to the most recent AA7075 research, mechanical parameters, including tensile as well as yield strength, improved by 33.8% and 13.56% when the basic material was reinforced with titanium boride ($TiB_2$). Nearly 10% more hardness can be achieved by incorporating ceramic-based strengthening like SiC into the aluminium matrix [23–25]. These self-lubricating aluminium mixtures were produced employing the powder metallurgy approach in the field of Al matrix [26, 27]. The mechanical and tribological characteristics of this nanostructured composite are enhanced by the inclusion of graphene up to 5% weight. By reinforcing silicon carbide and alumina particles with composites, the researcher has examined aluminium alloys based on structure, including AA6061 and AA7075. When mechanical characteristics like tensile properties and hardness and tribological characteristics like wear loss are concerned, both composite samples exhibit a noticeable improvement [28]. As a result, the density of samples has reached the expected level [29, 30]. Many characteristics, such as granular dimensions, wt. % of strengthening, applying load, distance as well as speed and industrial technique, were shown to influence the wear performance of Al composites [31, 32].

Growing the volume portion of strengthening declines the wear rate, while raising the particle size does the opposite. Due to correct precipitation and effective hardening, the composite used with age treatment will have better wear resistance [33, 34]. When brake pads are used, the tribo-layer generated on the pin material during the wear test has a greater impact on wear behaviour. It is apparent that the aluminium alloy with ceramic and metallic particle strengthening increases properties, as well as composite density when compared to the basic aluminium alloy [35–37]. The corrosion behaviour of these aluminium alloys in diverse media has received just a few research information. In light of this, the most pertinent information has been provided [38, 39]. Aluminum alloy AA6061 corrosion behaviour in acidic and alkaline environments at various concentrations and temperatures has been examined. Tafel polarisation and impedance spectroscopy were used in the electrochemical techniques used in the experiment (EIS) [40]. The results reveal that the AA6061 aluminium alloy is more susceptible to corrosion in alkaline media (NaOH) than in acidic media (Ph). AA6061 aluminium alloy with an alumina-based composite has been studied in salt water, acidic, and alkaline media conditions [41, 42]. Corrosion resistance of the composite is superior to that of other media in salt water, although the unreinforced state is superior in acidic and alkaline environments. Both reinforced and unreinforced aluminium alloys demonstrate improved corrosion resistance after heat treatment [43–45]. A passive oxide layer has been found to improve corrosion resistance when applied to heat-treated AA6061 with silicon carbide reinforcement, according to earlier research.

The best wear process parameter for various operating conditions was also identified. The effects of grain size, weight, and sliding distance were studied using a factorial design of experiments. SiC emery broadside wear rate improved with rising applied load, coarse magnitude, and distance, while $Al_2O_3$ paper wear rate decreased only with decreasing sliding distance. The material's rate of wear was altered in a number of ways by the variables. Another study on Al—5% SiC found that the applied load is the most critical factor when using Taguchi's $L_{27}$ orthogonal arrangement strategy and increased wear resistance using SiC strengthening in an aluminium matrix. Taguchi's $L_{27}$ orthogonal arrangement design (Al/SiC/Gr) was active in examining the ideal wear constraint of a hybridized aluminium composite (Al/SiC/Gr), which was established by ANOVA. The sliding distance (57.12%) was shown to be the most important process factor in the study. $L_{27}$ orthogonal arrangement plan and the analysis of variance were utilised to optimize an Al-based composite strengthened with 5–15% SiC. The sliding distance (49.12%) is the most significant processing factor that influences wear. By means of Taguchi's $L_{27}$ design and ANOVA, a structure-based hybrid aluminium alloy (AA6061) composite was discovered to have the best wear rate and frictional coefficient.

The best wear rate and coefficient of friction can be attained by using a variety of processing factors, including 4.5 m/s sliding speed, 15 N applied load, 20 minute sliding time, and 15% reinforcement. By investigating how reinforcement content (measured as a percentage of volume) affects qualities, this investigation also sought to identify the optimal value with the greatest impact on specimen tribological characteristics including rate of wear and frictional coefficient. The most crucial parameter does not have a name. An examination of the literature reveals that metallic-derived reinforcement alone or in grouping with ceramic-derived reinforcement has received relatively little research attention. Ceramic and metallic reinforcements can be added to aluminium matrix for the purpose of this investigation. Since ceramic particles in metal matrix increase the rate of wear and frictional coefficient as well as the hardness and strength of the material, this is a good reason to incorporate metallic reinforcement. With metallic reinforcement, a composite's impact strength improved without sacrificing any of the material's structural integrity [31–40].

An experiment's planning, design, and analysis are all covered by this statistical technique. To determine the best answer, the design of experiment method is employed. Systematic design, factor design, and lenience design are all stages in the optimization process. The wear testing in our study was made more efficient by the use of parameter design. Designing optimum process parameters and determining product parameters based on optimal processing factor values is a key part of the parameter designing process. The Taguchi approach is a powerful tool for determining the optimum strategy with high-quality structures from a range of design of experimental methods. It is a usual practise to do a large number of experiments in which just one variable is changed while the other remains constant. Using the Taguchi technique, fewer experiments are required to get an optimum answer. The Taguchi method allows for the interplay of several factors. As a result of the aforementioned principles, the Taguchi technique outperforms conventional experimentation [40–45]. Minitab-16 software was used to name all the data, and ANOVA was used to generate the percentages. Thus, this work aims to fabricate the aluminium composite reinforced with ceramic and metallic fibres and to study its various characterization including physical, corrosion, and wear behaviour.

## 2. Experimental Procedure

*2.1. Material Details.* The ingot is melted at 750°C in a muffle furnace for 45 minutes with AA6061 raw material, as shown in Figure 1 in a graphite crucible, weighing 700 g. An AA6061 is a class of metal that seems to have a high strength-to-weight proportion and may be heat-treated. It is utilised in industrial and structural applications due to its excellent mechanical properties. After that, the strengthening was heated in a different furnace for about an hour at 500°C for silicon nitride, whose composition is shown in Table 1 and for about 15 minutes at 100°C for copper nitrate. The primary goal of heating and strengthening is to reduce the humidity and improve the blend of the reinforcement with the composites. Oxygen from the dispersoid surface was scavenged by 2 wt. % pure magnesium, thinning the gas layer and improving moistening and response-aided moistening with the dispersoid surface. Owing to the continual exciting action of a multiblade stirrer inside the furnace, stir casting provided a standardized dispersion of fortification in the composites. At 300 rpm, the stirrer was running for 15 minutes, and the processing parameters are shown in Table 2. The molten fluid was then poured into a 120 mm long by 25 mm wide heated metal mould. The composite sample was removed from the mould once it had cooled to room temperature.

## 3. Testing Details

*3.1. Tensile Test.* Copper (Cu $(NO_3)_2$) and silicon ($Si_3N_4$) were used to reinforce the aluminium composite with different weight percentages, but the final product was successful. To achieve the standard subsize dimension, the cast specimens were CNC machined. In accordance with the ASTM E8/E 8M-08 B557 standard, the tensile strength of the composite was measured using an electronic tensile testing machine. The experimentation was conducted at room temperature.

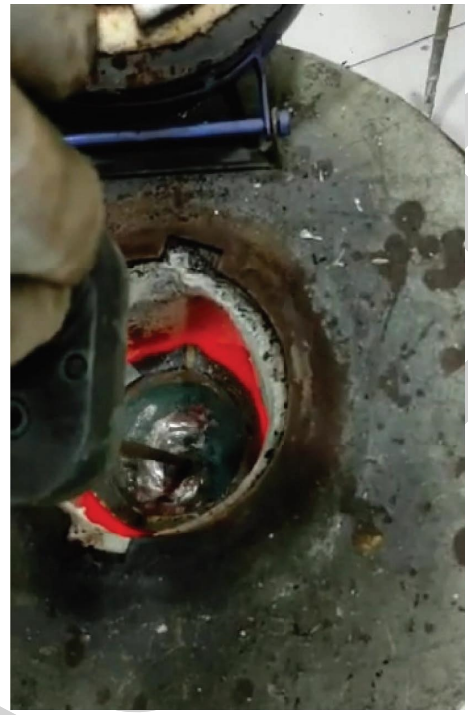

Figure 1: Stir casting process.

*3.2. Hardness Test.* An indentation is used to measure a metal's resistance to plastic deformation. In order to calculate the impact of metallic strengthening on the mixture specimen's hardness, the macro of the specimen was subjected to a Brinell hardness test. 10 mm ball was loaded with 500 kg and held for 20 s in Brinell hardness. Macrohardness testing, as shown in Figure 2 was performed using the specimen, which was produced in accordance with ASTM E10.

*3.3. Impact Test.* A material's impact strength measures its capacity to withstand a sudden application of force. A composite specimen was subjected to the IZOD impact test. A $66 \times 12.8 \times 3.4$ mm cast specimen was CNC machined to measure the entire energy fascinated by the composite specimen. The experiment was conducted at room temperature. According to ASTM D256, the specimen was created.

*3.4. Salt Spray Test-Corrosion Test.* The corrosion performance of the composite specimen was examined using the ASTM B117-2011 salt spray method. An accelerated corrosion test known as the salt spray test (fog test) is employed to determine the corrosion resistance of constituents to salt spray or salt fog at raised temperatures. As part of the salt spray testing process, a salt water solution is continually

Table 1: Characteristics of reinforcements.

| Reinforcement particles | Average particle size ($\mu$m) | Hardness (GPa) | Density (g/cm$^3$) | Melting point (°C) |
|---|---|---|---|---|
| Silicon nitride | 10–40 | 34.8 | 4.32 | 2150 |
| Copper nitrate | 10–40 | — | 4.36 | 150 |

Table 2: Stir casting processing factors.

| Processing factors | Values |
|---|---|
| Stirring time | 20 min |
| Molten composite temperature | 750°C |
| Preheated temperature of permanent mould | 720°C |
| Stirring speed | 350 rpm |
| Preheated temperature of Cu $(NO_3)_2$ | 120°C soaking time 20 min |
| Preheated temperature of $Si_3N_4$ | 750°C soaking time 60 min |

applied to test specimens in a surrounding salt spray testing system or chamber. As the test progressed, the environment that had been created was maintained. The weight loss technique was employed to calculate the corrosion rate of each sample. An electronic weighting device with a precision of 0.1 mg was used to determine the specimen's weight prior to testing. Weighing and cleaning were then completed to ascertain the specimen's weight. We utilise the Table 3 in this situation.

*3.5. Pin-on-Disc Test.* Wear tests were executed in accord with the ASTMG99 in dry, unlubricated sliding conditions. Pinned-on-disc wear testing was utilised to determine these parameters in Figure 3. The composite was used to make a cylinder-shaped pin with a width of 10 mm and a span of 25 mm. EN32 steel with an HRC65 hardness was used to make the discs. $L_{27}$ Taguchi orthogonal design was used to improve the process parameters. The frictional coefficient, wear rate, and wt. % reinforcement are all impacted by the same processing parameter. Table 4 lists the processing factor levels. An analysis of variance was employed to calculate the statistical significance of the different factors and the interactions among them.

## 4. Result and Discussion

*4.1. Density and Porosity.* Table 5 shows the results of density and porosity. Electronic weighing equipment with a 0.1 mg resolution was utilized to measure the experimental density using a composite sample of 60 mm height and 9.5 mm diameter. Density of AA6061 reinforced with 12 wt. % $Si_3N_4$ and different percentages of metallic reinforcement $Cu(NO_3)_2$ are shown. A general impression is that the density of materials grew as the percentage of metallic reinforcement varied. With 12 wt. % $Si_3N_4$ reinforcement and 6 wt. % $Cu(NO_3)_2$, a sample with the combined state is more dense than the sample with 12 wt. % $Si_3N_4$ reinforcement and no $Cu(NO_3)_2$ with 3.26338 g/cm$^3$ density. To increase the density of a composite, metallic materials are added to a lower-density material. Composite matrix porosity decreased when metallic strengthening engaged the space vacated by the insertion of metallic reinforcement. Because of this, the volume or compactness of the composite, measured by the number of atoms, has grown.

Figure 2: Hardness tester.

Table 3: Salt spray analysing factor.

| Test factors | Values |
|---|---|
| Solution pH value | 6.5–6.95 |
| Sample loading position in the chamber | 45° angle |
| Concentration of solution | 4.9–5.6% of NaCl |
| Chamber temperature | 35.6–36.8°C |
| Volume of salt solution collected | 1.2–1.5 ml/hr |
| Air pressure | 15–19 psi |

Magnesium-based binders have been shown to increase the wettability and lower the threshold pressure for strengthening, therefore increasing the strong contact between the matrix and the particles. Increasing density and decreasing porosity levels are the result of this. With (1), it is possible to determine the composite's density.

$$\rho_C = \rho_m \varphi_m + \rho_r \varphi_r, \quad (1)$$

where $\rho_C, \rho_m$, and $\rho_r$ are the density of composites, matrix, and reinforcement correspondingly.

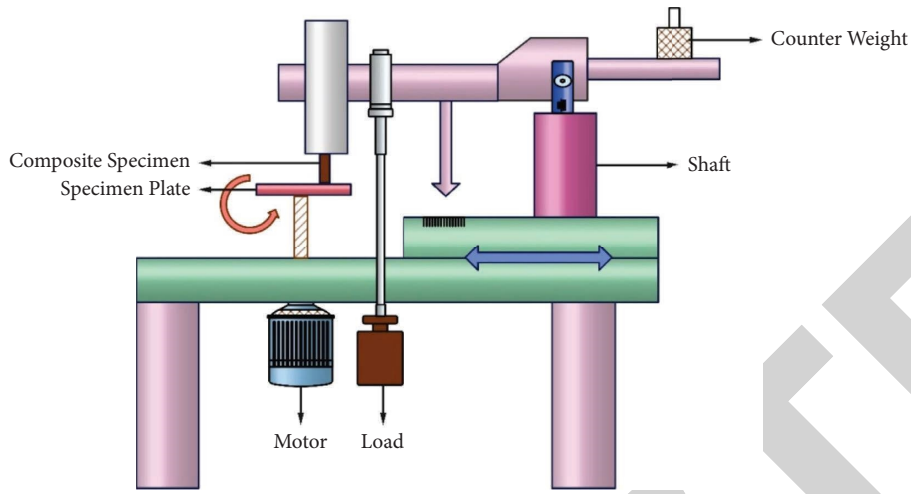


Figure 3: Diagram of pin-on-disc.

Table 4: Control factors and its levels.

| Control factors | Levels | | |
|---|---|---|---|
| | 1 | 2 | 3 |
| A: copper nitrate reinforcement (wt. %) | 3 | 6 | 9 |
| B: applied load (Newton) | 15 | 20 | 25 |
| C: sliding distance (metre) | 1250 | 1750 | 2250 |
| D: sliding speed (revolution per minute) | 250 | 350 | 450 |

Table 5: Density and porosity for variant reinforcement.

| Wt. % reinforcement of copper nitrate | Theoretical density ($g/cm^3$) | Experimental density ($g/cm^3$) | Porosity (%) |
|---|---|---|---|
| 0 | 3.6834 | 3.843 | 4.61 |
| 3 | 3.8714 | 3.781 | 3.53 |
| 6 | 3.7438 | 3.678 | 3.70 |
| 9 | 3.6412 | 3.618 | 3.72 |

Equation (2) was used to determine the sample's porosity

$$\text{Porosity} = \frac{\rho_T - \rho_E}{\rho_T} \times 100\%, \quad (2)$$

where $\rho_T, \rho_E$ are theoretical and experimental density of composites correspondingly

### 4.2. Mechanical Properties

*4.2.1. Macrohardness.* Density and hardness have a mathematical relationship that is proportionate to one another. Soft base material is hardened by adding of copper nitrate, which acts as a "hard phase." Plastic distortion theory states that the accumulated displacement increases as foreign particles such as reinforcements, are added. As a result of the reinforcing, composites now have a higher hardness rating. To further improve composite material resistance to penetration, up to 9 weight% of reinforcing steel is added to the matrix for better macrohardness. Figure 4 shows the connection between the % of metallic strengthening and the hardness value. By increasing the amount of metallic nitrate in the matrix, the hardness of the composites is decreased. Adding more metallic nitrate has no effect on its solubility or reactivity. Consequently, the toughness of the hybrid composite with 9% copper nitrate is superior.

*4.2.2. Tensile Strength.* Synthesized aluminium hybrid composites with varied weight percentages of metallic reinforcement are shown in Figure 5 to have a positive connection with tensile strength. Initially, the composites with 12% $Si_3N_4$ was 254 MPa in initial tensile strength. The tensile strength of the matrix has grown to 268 MPa following the addition of copper nitrate metallic reinforcement. Hard metallic reinforcement is present at the grain boundary to increase the tensile strength, and this causes the dislocation to pile up with the grains. As a result, the matrix's internal resistance and carrying capacity have both increased. To summarise, the results show that copper nitrate constrains the dislocations in a soft matrix, changing its plastic deformation behaviour. Up to 9 weight % of dislocation density can be attributed to this phenomena. Up to 9% ceramic nitrate can be used as an additional metal nitrate reinforcement to improve both the tensile strength and hardness of a material, according to this study. In the

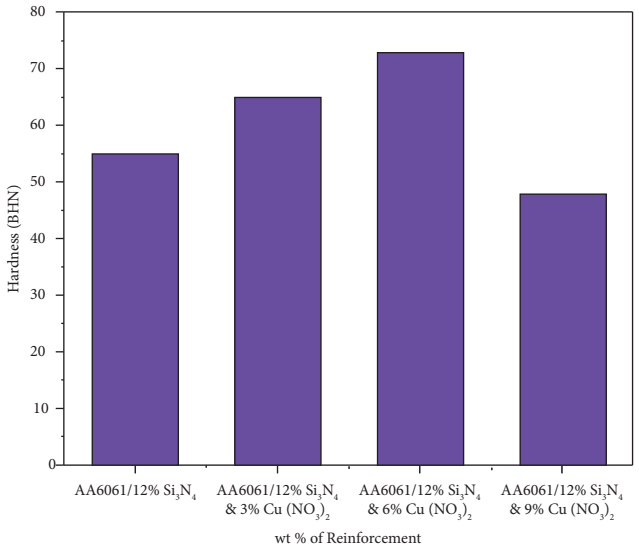


Figure 4: Variation in macrohardness as a function of Cu $(NO_3)_2$ weight percentage.

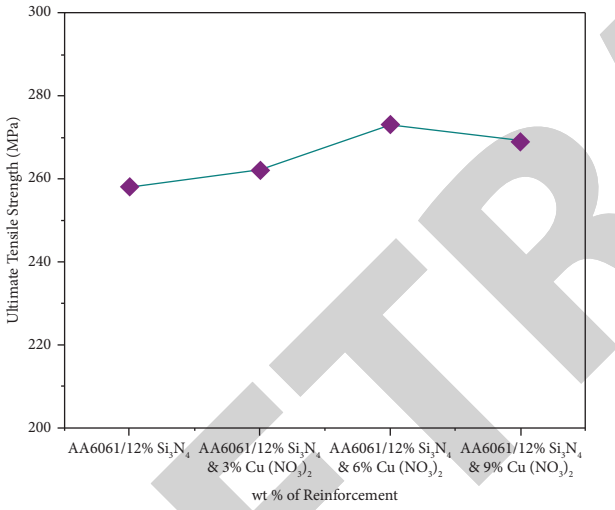


Figure 5: Tensile strength varies depending on the weight fraction of $Cu(NO_3)_2$.

presence of additional metallic reinforcement, the soft phase expands, but the mechanical qualities remain unchanged. Hybrid composite containing 9 weight % copper nitrate has virtuous wear and mechanical characteristics.

Hence, the improved performance and characteristics of the hybrid composite with 9 weight % copper nitrate. Samples with increasing or decreasing amounts of reinforcement are shown in Figure 6. Compared to 0, 3, 6, 9 wt. % Cu $(NO_3)_2$, the composite with 8 wt. % Cu $(NO_3)_2$ mixed together with AA6061/12 wt. % $Si_3N_4$ exhibits lower ultimate stress. The specimen's wear and friction characteristics rise as the tensile strength increases. As a result, the optimal amount of Cu $(NO_3)_2$ in the composite was 6%. Composite failure is caused by void nucleation and its coalescence, which disrupts the matrix-reinforcement relationship, resulting in composite failure.

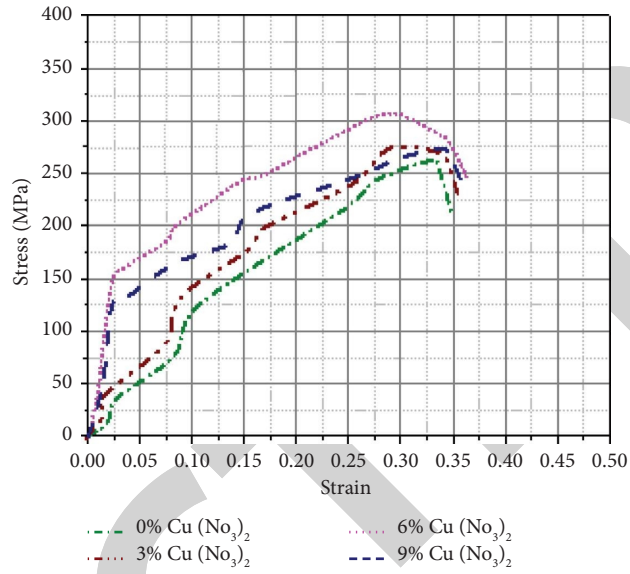


Figure 6: Stress—strain for different wt. % of Cu $(NO_3)_2$.

*4.2.3. Impact Strength.* Composites based on AA6061 have been utilised widely in an extensive range of fields, including ballistics, corrosion, the harshest environments, and heavy-duty applications. According to ASTM specifications, a CNC milling machine was used to cut and process the plate into the V-notch specimen. The notch angle and cross-sectional area were both set to 10 $mm^2$. Unreinforced AA6061's impact strength is superior to that of reinforced composite, as shown by the instrumental impact test. The unstrengthened squeeze out AA6061 alloy has an impact strength of 92 Joule at atmospheric temperature, but the strengthened AA6061 alloy with 12 wt. % silicon nitrate has a strength of just 5 J.

The composite impact strength and weight percentage of metallic reinforcement are shown in Figure 7. This is due to the reinforcement being grouped or agglomerated in places where crack nucleation and propagation are more likely to occur. Due to its lower energy absorption than an unreinforced alloy, the AA6061 ceramic-reinforced composite eventually fractures. Cracking and decohesion at particle interfaces also lead to fast microcrack growth and reduced impact strength.

*4.2.4. Corrosion.* The salt spray method was used to examine the corrosion behaviour of AA6061 reinforced with ceramic and metal. The weight loss technique and physical reflection on the visible outward of the specimen were used to analyse the behaviours. The strengthened AA6061 was subjected to a salt spray test. Even after 36 hours, there is no evidence of rust on the sample surface. It was only after 48 hours of exposure that the rust began to appear. Since the corrosion process begins after only 48 hours of exposure, it can be deduced that using copper nitrate as an additional metallic reinforcement has a significant impact on weight reduction.

Copper nitrate reinforcement has improved the composite's corrosion resistance. The copper metal's passive behaviour is whether helps the AA6061-based composite resist corrosion. In comparison, the corrosion resistance is

improved, owing to the occurrence of copper nitrate elements. Indeed, the occurrence of corundum file (Alumina) on the aluminium alloys' surfaces, as well as the presence of copper, has improved corrosion resistance in all environmental conditions. Few studies in the literature have shown that the presence of copper in aluminium alloys improves corrosion resistance. The outcome of the salt spray test is indicated in Figure 8. Table 6 displays the results of the corrosion tests. The following was used to compute the sample corrosion rate:

$$\text{Corrosion rate (mmpy)} = \frac{8.75 \times 10^4 \times \text{weight loss (gm)}}{\text{Composite density}\left(\text{gm/cm}^3\right) \times \text{Exposed area}\left(\text{cm}^2\right) \times \text{Exposuretime (hr)}}. \quad (3)$$

*4.2.5. Mechanism of Wear Test.* Table 7 shows wear test of produced composites. Hybrid composite pins of various compositions were exposed to dry sliding wear trials with diverse loads, such as 15 N, 20 N, and 25 N. At speeds of 250 rpm, 350 rpm, and 450 rpm, a sliding distance of 1250 m, 1750 m, and 2250 m was achieved. Prior to testing, the end surface of the test sample is smooth and refined with a metallographic alloy. To remove any residues of composite from the specimen and counter face disc, acetone was used. Weighing the specimen earlier and afterwards testing and getting an accurateness of 0.1 mg can be used to compute the wear loss. The normal load was used to calculate the frictional coefficient, while the data acquisition system provided the tangential load. Five times each test was performed before the average value was calculated and examined. Reinforced AA6061/12 wt $Si_3N_4$ with 3, 6, or 9 wt. % for unreinforced AA6061 The roughness of the surface 0.279 m, 0.406 m, 0.39 m, and 0.386 m were measured using the Ra-value using the surface roughness tester. On the worn surface, counter face pits allowed us to see the microcutting and microplowing that had occurred. abrasive and adhesive damage is indicated by the appearance of a plough mark and a crack. There is a crack in the material due to the weakening of the reinforcement-to-matrix linkage as load and sliding distance increase. The main output is the response function's average value at a specified parameter level. The S/N (Signal/Matrix) ratio is used to determine the parameter's quality attributes. First, smaller is preferable in terms of size. Second, higher is better. Third, nominal is best in order to achieve the best quality attributes, we adopted the smaller-is-better principle to preserve less wear loss and friction. The S/N ratio was obtained by transforming the loss function logarithmically, as illustrated in the relationships inthe following equation:

$$\frac{S}{N} = -10 \log \frac{1}{n}\left(\epsilon_{y^2}\right), \quad (4)$$

where $n$ = no. of observation and $y$ = experiment.

*4.3. Impact of Testing Factors on Wear Loss.* To illustrate the relationship among various process variables and the wear and frictional coefficients of the composites, shown in Figures 9(a) and 9(b). For example, if a process parameter's mean plot graph curve is close to the horizontal and it has no effect on composites, then it has a bigger impact. It was revealed that the difference in the mean S/N ratio between its highest and lowest values was the most important control parameter. S/N ratios that are more than two standard deviations off of a given value should be used as controls. A decreased wear rate and a better sound-to-noise coefficient of friction were used to analyse the process parameter in this investigation. Testing elements like the wt. % of reinforcement, applying load, distance as well as speed were examined employing the Taguchi method. That which was most crucially derived from the analysis of variance. The significance level was chosen at 5% with a 95% confidence interval. Because of the strong wear resistance of the metallic reinforcement, the weight percentage of reinforcement ($p$ = 35.68%) had the greatest impact on wear loss, as indicated in Table 8. $Cu(NO_3)_2$ and $Si_3N_4$ strengthen the surface, making it extremely hard and durable. Wear rate falls as reinforcement percentage increases, so this is why. Wear loss was influenced by sliding distance, speed, and applied load ($p$ = 29.16 and 22.04%, respectively). Weight % reinforcement and applied load (3.10%) and weight % reinforcement and sliding distance (−2.6%) only have a minimal impact on composite's wear rate (−2.04%).

*4.4. Impact of Testing Factors on the Friction Coefficient.* Table 9 displays the ANOVA results for friction coefficient. Nearly 73.22% of the coefficient of friction was impacted by the weight percentage of metallic reinforcement. There was a 9.647% influence from the sliding distance. Other parameter interactions, such as the load applied and the sliding velocity, were not considerably altered. By means of the weight proportion of strengthening rises, so did the coefficient of friction. There is a pooled error of 9.647% in the ANOVA table related to the results. If you want to know how much variation there is in the mean and variance, you can use this approach. This method uses absolute numbers instead of unit values. According to the interaction of variables, the friction coefficient of hybridized MMC is significantly influenced (4.56%) by the interplay of load and reinforcing percentage.

*4.5. Confirmation Test.* Using a linear equation, it is possible to evaluate the relationship among two or more forecast values and responsible variables. Calculating the wear rate and friction coefficient of hybrid composites can be done by utilising equations. It has a regression coefficient of 0.88. A positive load indicator implies that the composite's wear

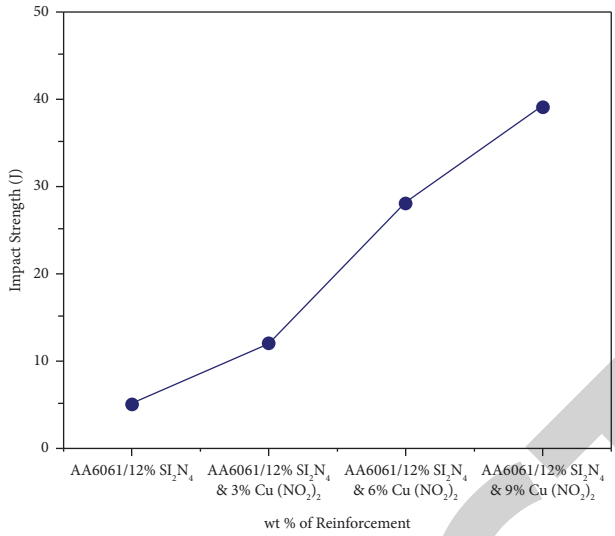


Figure 7: Impact strength varies with Cu $(NO_3)_2$ weight percentage.

Table 6: Composites with differing levels of reinforcement possess varying rates of corrosion.

| Wt. % of reinforcement of copper nitrate | Starting weight (gm) | Ending weight (gm) | Weight loss (gm) | Density ($g/cm^3$) | Corrosion rate (mmpy) |
|---|---|---|---|---|---|
| 0 | 2.6127 | 2.9612 | 0.0070 | 2.1624 | 0.98251 |
| 3 | 2.4512 | 2.4768 | 0.0039 | 2.9624 | 0.58942 |
| 6 | 2.4316 | 2.6313 | 0.0035 | 2.2710 | 0.04342 |
| 9 | 2.1496 | 2.787 | 0.0020 | 2.7891 | 0.23946 |

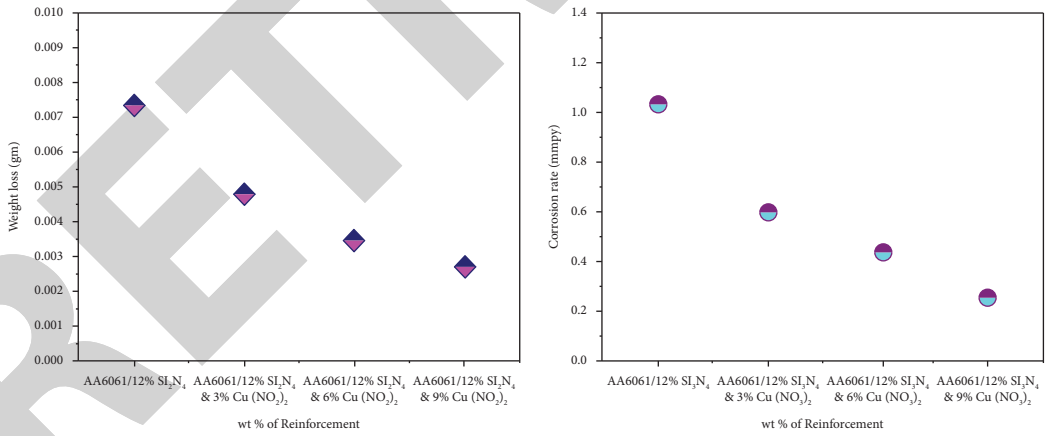


Figure 8: (a) Weight loss vs wt. % of metallic reinforcement and (b) corrosion rate vs wt. % of metallic reinforcement.

rate and friction coefficient will increase. When the speed increases, the wear rate of composites declines, according to the regression equation. The friction coefficient is reduced by increasing the weight percentage of the reinforcing component. Hybridized composites' abrasion resistance and load carrying capacity both rose as the reinforcing weight percentage increased. Mathematical modelling and experimental reference process parameter values were compared to see if their comparison would affect the processing factor expected to be affected by it. As shown in Table 10, these numbers are broken out. The wear loss and friction coefficient were evaluated. From 8.4% to 11.42%, the wear rate and friction coefficient inaccuracy percentages were found.

Table 7: $L_{27}$ orthogonal arrangement considered by Taguchi.

| Ex. no | A | B | C | D | Wear loss (gm) | S/N ratio (db) | Friction coefficient | S/N ratio (db) |
|---|---|---|---|---|---|---|---|---|
| 1 | 3 | 15 | 1250 | 250 | 0.0050 | 46.0206 | 0.6984 | 3.11792 |
| 2 | 3 | 15 | 1750 | 350 | 0.0062 | 44.1522 | 0.7632 | 2.34723 |
| 3 | 3 | 15 | 2250 | 450 | 0.0058 | 44.7314 | 0.7585 | 2.40089 |
| 4 | 3 | 20 | 1250 | 350 | 0.0048 | 46.3752 | 0.6755 | 3.40749 |
| 5 | 3 | 20 | 1750 | 450 | 0.0059 | 44.5830 | 0.7764 | 2.19829 |
| 6 | 3 | 20 | 2250 | 250 | 0.0102 | 39.8280 | 0.7653 | 2.32337 |
| 7 | 3 | 25 | 1250 | 450 | 0.0059 | 44.5830 | 0.6958 | 3.15031 |
| 8 | 3 | 25 | 1750 | 250 | 0.0091 | 40.8192 | 0.6859 | 3.27478 |
| 9 | 3 | 25 | 2250 | 350 | 0.0140 | 37.0774 | 0.7625 | 2.35520 |
| 10 | 6 | 15 | 1250 | 350 | 0.0061 | 44.2934 | 0.5582 | 5.06420 |
| 11 | 6 | 15 | 1750 | 250 | 0.0069 | 43.2230 | 0.5826 | 4.69259 |
| 12 | 6 | 15 | 2250 | 250 | 0.0108 | 39.3315 | 0.6831 | 3.31031 |
| 13 | 6 | 20 | 1250 | 350 | 0.0073 | 42.7335 | 0.6101 | 4.29198 |
| 14 | 6 | 20 | 1750 | 250 | 0.0090 | 40.9151 | 0.6913 | 3.20667 |
| 15 | 6 | 20 | 2250 | 450 | 0.0124 | 38.1316 | 0.6685 | 3.49797 |
| 16 | 6 | 25 | 1250 | 250 | 0.0092 | 40.7242 | 0.6861 | 3.27225 |
| 17 | 6 | 25 | 1750 | 350 | 0.0121 | 38.3443 | 0.6586 | 3.62757 |
| 18 | 6 | 25 | 2250 | 450 | 0.0135 | 37.3933 | 0.7952 | 1.99047 |
| 19 | 9 | 15 | 1250 | 450 | 0.0043 | 47.3306 | 0.3249 | 9.76501 |
| 20 | 9 | 15 | 1750 | 250 | 0.0068 | 43.3498 | 0.5604 | 5.03004 |
| 21 | 9 | 15 | 2250 | 350 | 0.0125 | 38.0618 | 0.5826 | 4.69259 |
| 22 | 9 | 20 | 1250 | 250 | 0.0118 | 38.5624 | 0.4624 | 6.69964 |
| 23 | 9 | 20 | 1750 | 350 | 0.0142 | 36.9542 | 0.4363 | 7.20430 |
| 24 | 9 | 20 | 2250 | 450 | 0.0137 | 37.2656 | 0.4769 | 6.43145 |
| 25 | 9 | 25 | 1250 | 350 | 0.0118 | 38.5624 | 0.4658 | 6.63601 |
| 26 | 9 | 25 | 1750 | 450 | 0.0170 | 35.3910 | 0.5626 | 4.99601 |
| 27 | 9 | 25 | 2250 | 250 | 0.0178 | 34.9916 | 0.4649 | 6.65281 |

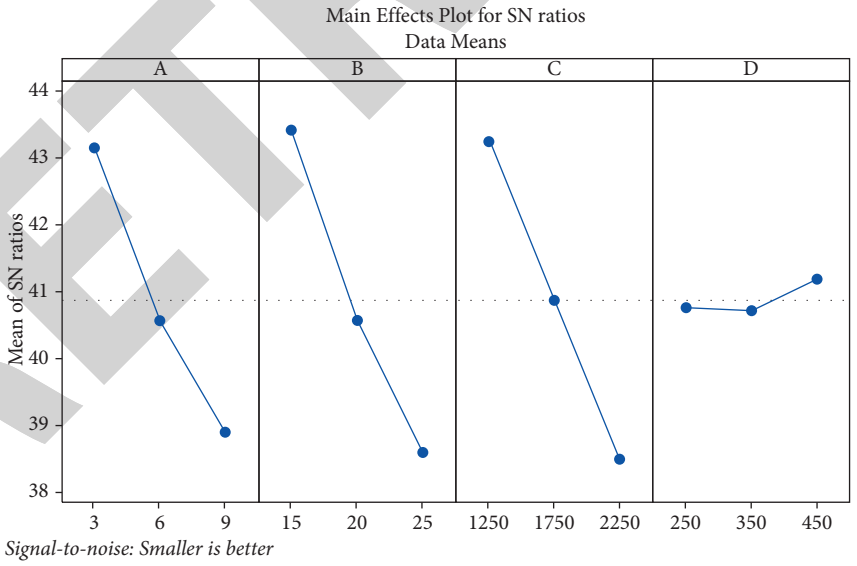


(a)

Figure 9: Continued.

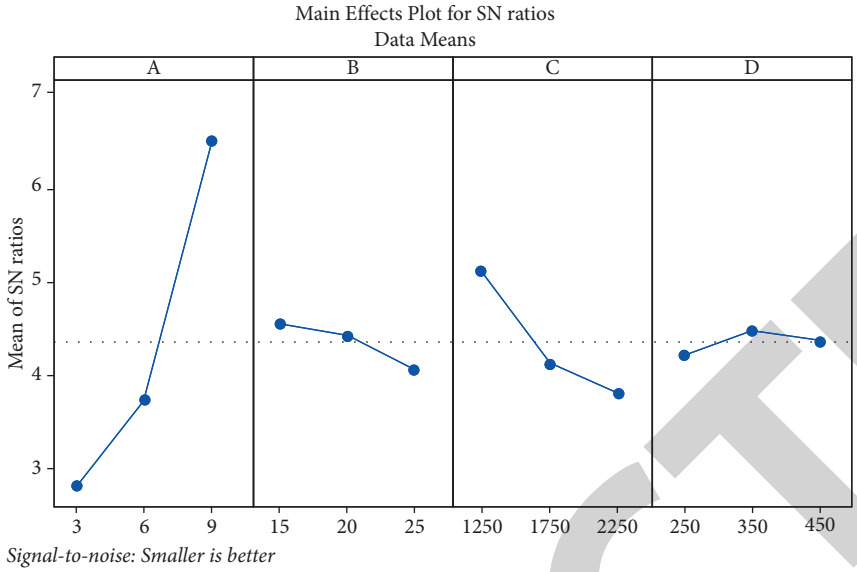


(b)

Figure 9: Main effect of plot for sound to noise ratio (a) wear rate (b) coefficient of friction.

Table 8: ANOVA for wear loss, employing adjusted SS for tests.

| Source | DoF | SS | Adjusted sum of squares | Adjusted mean of squares | *F*-ratio | *p*-value | % of contribution |
|---|---|---|---|---|---|---|---|
| A | 2 | 0.000154 | 0.000154 | 0.000077 | 41.23 | 0.001 | 32.835 |
| B | 2 | 0.000119 | 0.000119 | 0.000059 | 37.57 | 0.0002 | 27.624 |
| C | 2 | 0.000102 | 0.000102 | 0.000053 | 28.13 | 0.0002 | 24.135 |
| D | 2 | 0.000017 | 0.000017 | 0.000009 | 6.42 | 0.051 | 4.931 |
| A × B | 4 | 0.000011 | 0.000011 | 0.000005 | 3.94 | 0.159 | 3.598 |
| A × C | 4 | 0.000005 | 0.000005 | 0.000003 | 0.32 | 0.830 | −2.837 |
| B × C | 4 | 0.000002 | 0.000002 | 0.000002 | 0.41 | 0.869 | −2.162 |
| Error | 6 | 0.000012 | 0.000012 | | | | 11.876 |
| Total | 26 | 0.00043 | 0.00043 | | | | 100 |

Table 9: Analysis of variance for coefficient of friction, employing adjusted SS for tests.

| Source | DoF | ss | Adjusted sum of squares | Adjusted mean of squares | *F*-ratio | *p* value | Percentage of contribution |
|---|---|---|---|---|---|---|---|
| A | 2 | 0.057835 | 0.057835 | 0.023410 | 98.16 | 0.001 | 73.2201 |
| B | 2 | 0.004522 | 0.004522 | 0.002714 | 2.48 | 0.283 | 0.38946 |
| C | 2 | 0.020415 | 0.020415 | 0.010327 | 15.61 | 0.006 | 9.64725 |
| D | 2 | 0.000983 | 0.000983 | 0.000471 | 0.22 | 0.838 | −0.91842 |
| A × B | 4 | 0.010391 | 0.010391 | 0.005829 | 4.35 | 0.089 | 3.361241 |
| B × C | 4 | 0.004297 | 0.004297 | 0.002256 | 0.86 | 0.598 | 2.10426 |
| A × C | 4 | 0.003426 | 0.003426 | 0.001788 | 0.39 | 0.802 | 2.14856 |
| Error | 6 | 0.008436 | 0.008436 | 0.002125 | | | 10.04876 |
| Total | 26 | 0.339967 | 0.339967 | | | | 100 |

Table 10: Validation of the regression equation model by comparing it with experimental data.

| Exp. no | Experimental wear loss (gm) | Regression model wear loss (gm) | Error (%) | Experimental coefficient of friction | Regression model of coefficient of friction | Error (%) |
|---|---|---|---|---|---|---|
| 1 | 0.0052 | 0.00446 | 11.42 | 0.628 | 0.5933 | 5.26 |
| 2 | 0.0132 | 0.01158 | 8.4 | 0.569 | 0.5359 | 7.36 |
| 3 | 0.0184 | 0.01612 | 10.18 | 0.4654 | 0.4448 | 5.823 |

## 5. Conclusion

The following conclusions are deceased and are shown below in sequential order.

(i) Increased density and lower porosity were achieved by altering the proportion of metallic reinforcement in structure-based aluminium composites.

(ii) Once metallic strengthening is applied to the composites to prevent displacement motion, the hardness increases.

(iii) In comparison to unreinforced AA6061, the tensile strength of composite rose from 262 MPa to 279 MPa with altering weight percentage of metallic reinforcement.

(iv) Due to the accumulation of strengthening at grain boundaries, the impact strength of composites is lower than that of unreinforced base metals. However, the metallic reinforcement improved the composite's impact strength.

(v) Incorporating metal reinforcements increased the corrosion resistance of the structure-based aluminium composites.

(vi) With respect to wear loss, factors including weight percentages reinforcement, distance slid, load applied, and speed slid had an impact on how process parameters were prioritised.

## Data Availability

The data used to support the findings of this study are included within the article. Further data or information is available from the corresponding author upon request.

## Conflicts of Interest

The authors declare that there are no conflicts of interest regarding the publication of this paper.

## Acknowledgments

The authors appreciate the support from Arba Minch University, Ethiopia, for the research and preparation of the manuscript. The authors extend their appreciation to the Deanship of Scientific Research at King Khalid University, Kingdom of Saudi Arabia for funding this work through Large Groups Project under grant number: RGP. 2/162/43.

## References

[1] A. Sankhla and K. M. Patel, "Metal matrix composites fabricated by stir casting process–A review," *Advances in Materials and Processing Technologies*, vol. 8, no. 2, pp. 1270–1291, 2021.

[2] S. Narayan and A. Rajeshkannan, "Hardness, tensile and impact behaviour of hot forged aluminium metal matrix composites," *Journal of Materials Research and Technology*, vol. 6, no. 3, pp. 213–219, 2017.

[3] V. Mohanavel, K. Rajan, and M. Ravichandran, "Synthesis, characterization and properties of stir cast AA6351-aluminium nitride (AlN) composites," *Journal of Materials Research*, vol. 31, no. 24, pp. 3824–3831, 2016.

[4] A. Chaubey, P. Konda Gokuldoss, Z. Wang, S. Scudino, N. Mukhopadhyay, and J. Eckert, "Effect of particle size on microstructure and mechanical properties of Al-based composite reinforced with 10 vol.% mechanically alloyed Mg-7.4%Al particles," *Technologies*, vol. 4, no. 4, pp. 37-38, 2016.

[5] V. Mohanavel and M. Ravichandran, "Experimental investigation on mechanical properties of AA7075-AlN composites," *Materials Testing*, vol. 61, no. 6, pp. 554–558, 2019.

[6] H. C. Anilkumar, H. S. Hebbar, and K. S. Ravishankar, "Mechanical properties of fly ash reinforced aluminium alloy (Al6061) composites," *International Journal of Mechanical and Materials Engineering*, vol. 6, no. 1, pp. 41–45, 2011.

[7] S. Suresh Kumar and V. Mohanavel, "An overview assessment on magnesium metal matrix composites," *Materials Today Proceedings*, vol. 59, no. 2, pp. 1357–1361, 2022.

[8] T. S. Srivatsan and E. J. Lavernia, "Use of spray techniques to synthesize particulate-reinforced metal-matrix composites," *Journal of Materials Science*, vol. 27, no. 22, pp. 5965–5981, 1992.

[9] A. R. E. Singer and S. Ozbek, "Metal matrix composites produced by spray codeposition," *Powder Metallurgy*, vol. 28, no. 2, pp. 72–78, 1985.

[10] T. Sathish, S. D. Kumar, M. Ravichandran et al., "Waste food cans waste bamboo wood based AA8079/SS304/bamboo wood ash hybrid nanocomposite for food packaging," *Key Engineering Materials*, vol. 928, pp. 69–78, 2022.

[11] R. Tiwari, S. Sampath, B. Gudmundsson, G. Halada, C. R. Clayton, and H. Herman, "Microstructure and tensile properties of L12-Type NiCrAl alloy prepared by vacuum plasma spray forming," *Scripta Metallurgica et Materialia*, vol. 33, no. 7, pp. 1159–1162, 1995.

[12] J. A. Jeffrey, S. S. Kumar, P. Hariharan, M. Kamesh, and A. M. Raj, "Production and assessment of AZ91 reinforced with nano SiC through stir casting process," *Inside MS*, vol. 1048, pp. 9–14, 2022.

[13] V. Mohanavel and M. Ravichandran, "Influence of AlN particles on microstructure, mechanical and tribological behaviour in AA6351 aluminum alloy," *Materials Research Express*, vol. 6, no. 10, Article ID 106557, 2019.

[14] M. M. Ravikumar, S. S. Kumar, R. V. Kumar, S. Nandakumar, J. H. Rahman, and J. A. Raj, "Evaluation on mechanical behavior of AA2219/SiO2 composites made by stir casting process," *AIP Conference Proceedings*, vol. 2405, Article ID 050010, 2022.

[15] S. Gopalakrishnan and N. Murugan, "Production and wear characterisation of AA 6061 matrix titanium carbide particulate reinforced composite by enhanced stir casting method," *Composites Part B: Engineering*, vol. 43, no. 2, pp. 302–308, 2012.

[16] P. Sharma, S. Sharma, and D. Khanduja, "Production and some properties of Si 3 N 4 reinforced aluminium alloy composites," *Journal of Asian Ceramic Societies*, vol. 3, no. 3, pp. 352–359, 2015.

[17] K. M. Shorowordi, A. S. M. A. Haseeb, and J. P. Celis, "Velocity effects on the wear, friction and tribochemistry of aluminum MMC sliding against phenolic brake pad," *Wear*, vol. 256, no. 11, pp. 1176–1181, 2004.

[18] S. Ozden, R. Ekici, and F. Nair, "Investigation of impact behaviour of aluminium based SiC particle reinforced metal-matrix composites," *Composites Part A: Applied Science and Manufacturing*, vol. 38, no. 2, pp. 484–494, 2007.

[19] S. Basavarajappa and G. Chandramohan, "Dry sliding wear behavior of hybrid metal matrix composites," *Materials Science*, vol. 11, no. 3, pp. 253–257, 2005.

[20] A. Daoud and M. T. Abou El-khair, "Wear and friction behavior of sand cast brake rotor made of A359-20 vol% SiC particle composites sliding against automobile friction material," *Tribology International*, vol. 43, no. 3, pp. 544–553, 2010.

[21] S. B. Prabu, L. Karunamoorthy, S. Kathiresan, and B. Mohan, "Influence of stirring speed and stirring time on distribution of particles in cast metal matrix composite," *Journal of Materials Processing Technology*, vol. 171, no. 2, pp. 268–273, 2006.

[22] M. A. H. Howes, "Ceramic-reinforced MMC fabricated by squeeze casting," *Journal of the Minerals Metals & Materials Society*, vol. 38, no. 3, pp. 28-29, 1986.

[23] B.-K. Hwu, S.-J. Lin, and M.-T. Jahn, "Effects of process parameters on the properties of squeeze-cast SiCp-6061 Al metal-matrix composite," *Materials Science and Engineering*, vol. 207, no. 1, pp. 135–141, 1996.

[24] M. K. Surappa, "Aluminium matrix composites: challenges and opportunities," *Sadhana*, vol. 28, no. 2, pp. 319–334, 2003.

[25] M. K. Surappa and P. K. Rohatgi, "Preparation and properties of cast aluminium-ceramic particle composites," *Journal of Materials Science*, vol. 16, no. 4, pp. 983–993, 1981.

[26] L. Poovazhagan, K. Kalaichelvan, A. Rajadurai, and V. Senthilvelan, "Characterization of hybrid silicon carbide and boron carbide nanoparticles-reinforced aluminum alloy composites," *Procedia Engineering*, vol. 64, pp. 681–689, 2013.

[27] R. Keshavamurthy, S. Mageri, G. Raj, B. Naveenkumar, P. M. Kadakol, and K. Vasu, "Microstructure and mechanical properties of Al7075-TiB2 in-situ composite," *Research Journal of Material Sciences*, vol. 1, no. 10, pp. 6–10, 2013.

[28] W. Wang, Q.-y. Shi, P. Liu, H.-k. Li, and T. Li, "A novel way to produce bulk SiCp reinforced aluminum metal matrix composites by friction stir processing," *Journal of Materials Processing Technology*, vol. 209, no. 4, pp. 2099–2103, 2009.

[29] A. El-Ghazaly, G. Anis, and H. G. Salem, "Effect of graphene addition on the mechanical and tribological behavior of nanostructured AA2124 self-lubricating metal matrix composite," *Composites Part A: Applied Science and Manufacturing*, vol. 95, pp. 325–336, 2017.

[30] S. A. Kori and M. S. Prabhudev, "Sliding wear characteristics of Al-7Si-0.3Mg alloy with minor additions of copper at elevated temperature," *Wear*, vol. 271, no. 5–6, pp. 680–688, 2011.

[31] Y. Sahin, "Optimization of testing parameters on the wear behaviour of metal matrix composites based on the Taguchi method," *Materials Science and Engineering*, vol. 408, no. 1–2, pp. 1–8, 2005.

[32] B. M. Viswanatha, M. P. Kumar, S. Basavarajappa, and T. S. Kiran, "Effect of ageing on dry sliding wear behaviour of Al-MMC for disc brake," *Tribology in Industry*, vol. 36, no. 1, pp. 40–48, 2014.

[33] R. K. Uyyuru, M. K. Surappa, and S. Brusethaug, "Tribological behavior of Al-Si-SiCp composites/automobile brake pad system under dry sliding conditions," *Tribology International*, vol. 40, pp. 365–373, 2007.

[34] D. Prabhu and R. Padmalatha, "Studies of corrosion of aluminium and 6063 aluminium alloy in phosphoric acid medium," *International Journal of ChemTech Research*, vol. 5, no. 6, pp. 2690–2705, 2013.

[35] K. K. Alaneme and M. O. Bodunrin, "Corrosion behavior of alumina reinforced aluminium (6063) metal matrix composites," *Journal of Minerals and Materials Characterization and Engineering*, vol. 10, no. 12, pp. 1153–1165, 2011.

[36] K. K. Alaneme, "Corrosion behaviour of heat-treated Al-6063/SiCp composites immersed in 5 wt% NaCl solution," *Leonardo Journal of Sciences*, vol. 18, no. 18, pp. 55–64, 2011.

[37] S. Ghosh, G. Sutradhar, and P. Sahoo, "Wear performance of Al-5 %SiC metal matrix composites using Taguchi method," *Journal of Tribology and Research*, vol. 2, pp. 33–40, 2011.

[38] S. Basavarajappa and G. Chandramohan, "Wear studies on metal matrix composites: a taguchi approach," *Journal of Materials Science and Technology*, vol. 21, no. 6, pp. 845–850, 2005.

[39] V. C. Uvaraja and N. Natarajan, "Optimization of friction and wear behaviour in hybrid metal matrix composites using taguchi technique," *Journal of Minerals and Materials Characterization and Engineering*, vol. 11, no. 8, pp. 757–768, 2012.

[40] J. W. Kaczmar, K. Pietrzak, and W. Wlosiński, "The production and application of metal matrix composite materials," *Journal of Materials Processing Technology*, vol. 106, no. 1–3, pp. 58–67, 2000.

[41] P. Ravindran, K. Manisekar, P. Rathika, and P. Narayanasamy, "Tribological properties of powder metallurgy–Processed aluminium self lubricating hybrid composites with SiC additions," *Materials & Design*, vol. 45, pp. 561–570, 2013.

[42] G. B. V. Kumar, C. S. P. Rao, N. Selvaraj, and M. S. Bhagyashekar, "Studies on Al6061-SiC and Al7075-Al<sub>2</sub>O< sub>3</sub> Metal Matrix Composites," *Journal of Minerals and Materials Characterization and Engineering*, vol. 9, no. 1, pp. 43–55, 2010.

[43] S. C. Sharma, B. M. Girish, R. Kamath, and B. M. Satish, "Effect of SiC particle reinforcement on the unlubricated sliding wear behaviour of ZA-27 alloy composites," *Wear*, vol. 213, no. 1–2, pp. 33–40, 1997.

[44] R. N. Rao and S. Das, "Effect of matrix alloy and influence of SiC particle on the sliding wear characteristics of aluminium alloy composites," *Materials & Design*, vol. 31, no. 3, pp. 1200–1207, 2010.

[45] Y. Sahin, "Wear behaviour of aluminium alloy and its composites reinforced by SiC particles using statistical analysis," *and Design*, vol. 24, no. 2, pp. 95–103, 2003.